Supporting Information

Achieving ideal magnetic light emission with electric-type emitters

Ruizhao Yao[†], Hiroshi Sugimoto[‡], Tianhua Feng[§], Minoru Fujii[‡], Shimei Liu[†], Xinming Li[†], Sheng Lan[†], Guang-Can Li*[, †]

[†] Guangdong Provincial Key Laboratory of Nanophotonic Functional Materials and Devices, Guangdong Basic Research Center of Excellence for Structure and Fundamental Interactions of Matter, School of Optoelectronic Science and Engineering, South China Normal University, 510006 Guangzhou, China.

[‡] Department of Electrical and Electronic Engineering, Graduate School of Engineering, Kobe University, Rokkodai Nada, Kobe 657-8501, Japan.

[§] Department of Electric Engineering, College of Information Science and Technology, Jinan University, Guangzhou 510632, China.

1. Excitation of the magnetic dipole resonance of silicon nanoparticles with dipole emitters

The magnetic dipole resonance of a silicon nanoparticles can be excited by either electric or magnetic dipole emitters, depending on the where the dipole resides. As the magnetic fields associated with the MD mode are mainly trapped at the center of the particle, a magnetic dipole emitter at this site would most efficiently excite the MD mode (as shown in Fig. S1). Similarly, an electric dipole near the inner particle surface overlaps the MD-associated electric field hot spot and is able to excite the MD mode, too.

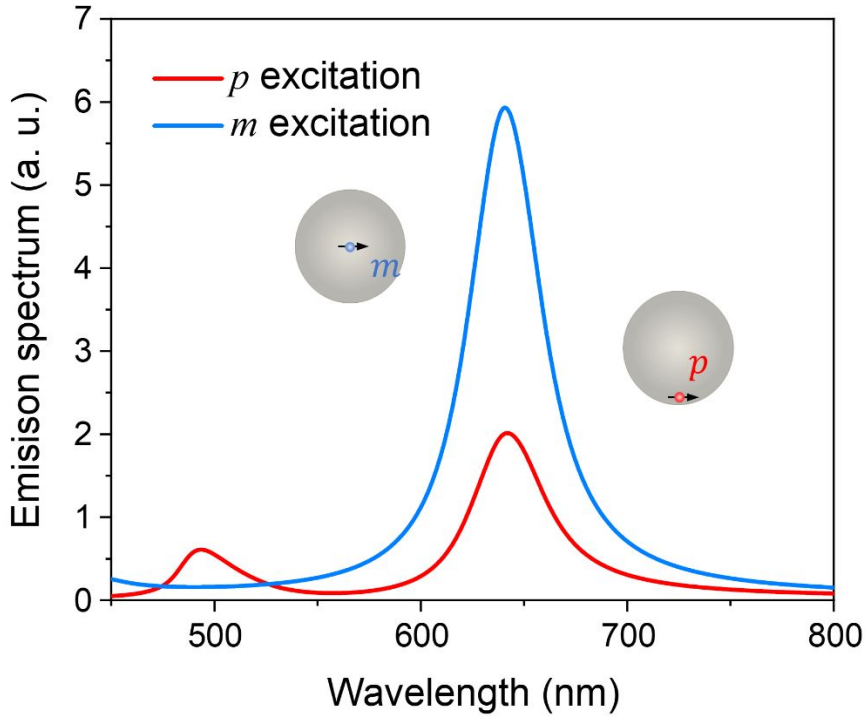

Figure S1. The emission spectra of a silicon nanosphere coupled to a magnetic dipole (m) emitter located at the particle center or electric dipole (p) placed 1 nm away from the inner particle surface.

2. The different coupling configurations of an electric dipole near silicon nanoparticles

An electric dipole oriented tangential to the surface of a Si nanoparticle can efficiently excite its magnetic dipole mode. But when the dipole is oriented along the surface norm, as shown in Fig.2Sa, it dominantly excites the ED-type particle mode, regardless of the presence of a dielectric substrate or not (Fig. S2b). When the surface-nearby electric dipoles have concurrent tangential and orthogonal components, the ED-type particle mode dominates the total excitation ($\delta_{md} \sim 39\%$, Fig. S2c) at the MD resonance wavelength. When such an orthogonal electric dipole pair is located inside the particle yet still close to the surface, the MD-type resonance dominates the total excitation ($\delta_{md} \sim 98.8\%$, Fig. S2d). This means; to achieve exclusive excitation of the MD-type particle resonance with an external electric dipole emitter, the emitter shouldn't have dipole component orthogonal to the particle surface.

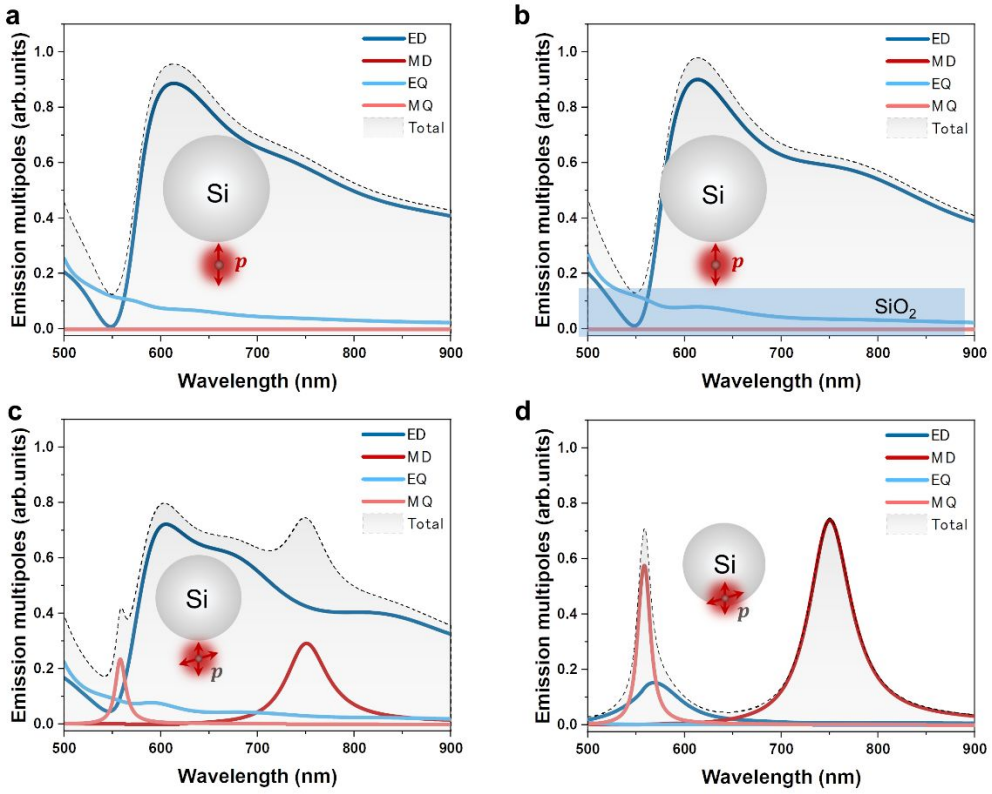

Figure S2. The coupling between the Si particle multipoles and an electric dipole with different orientations. (a, b) The emission multipoles of an electric dipole near the Si nanoparticle surface in air (a) or on a silica substrate (b), with the dipole moment oriented along the surface norm direction. The dipole-surface distance is 1 nm, and the particle-substrate separation distance is 2 nm. (c, d) The emission multipoles of a Si nanoparticle coupled to an electric dipole pair with concurrent tangential and orthogonal dipole orientations, located on either the out (c) or inner (d) side of the surface.

3. The scattering pattern at the MD resonance wavelength of a SiNS illuminated by plane wave

The scattering MD resonance of a Si nanoparticle illuminated by a plane wave contains contributions from both ED and MD multipoles, which can be resolved from its scattering patterns. As show in Fig. S3a, the far-field pattern of a pure MD source m_y exhibits the well-known doughnut-shaped pattern, with the dark axis, corresponding to the direction along which the radiation intensity is zero, aligned to the dipole axis (y). In contrast, for the plane wave (E_x polarized) illuminated Si nanoparticle, the scattering intensity along the dark axis is nonzero (Fig. S3b), which can be attributed to the excitation of the ED-type antenna mode.

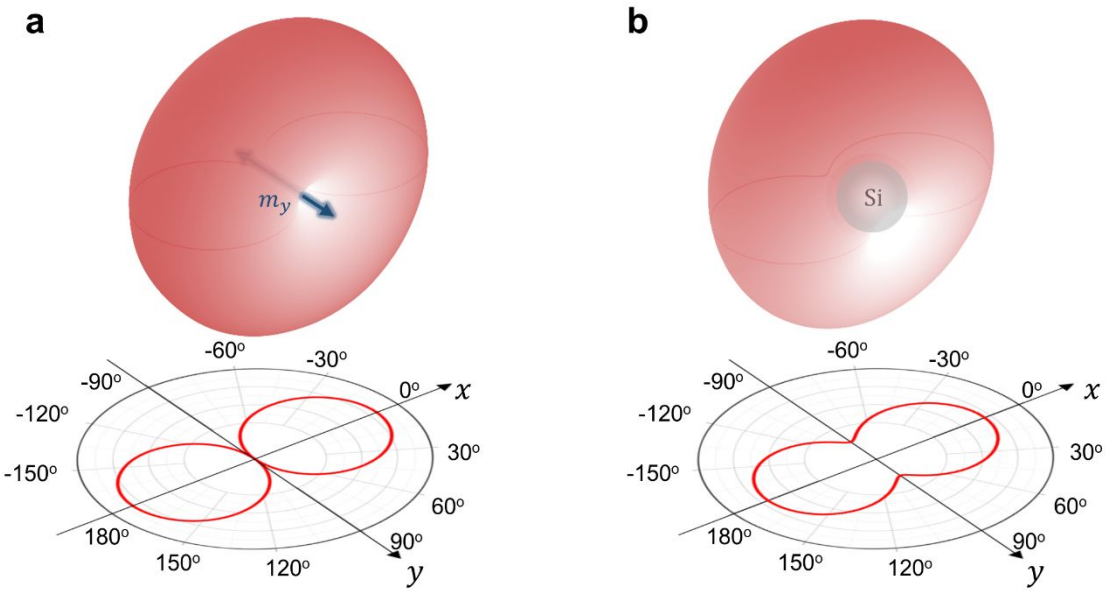

Figure S3. Comparison of the emission pattern of pure magnetic dipole in air (a) and the scattering pattern of a spherical Si nanoparticle (diameter 190 nm) illuminated by a plane wave (b). In simulation, the scattering wavelength is set at the magnetic dipole resonance of the particle (750 nm).

4. Analytical model for description of the scattering by a nanosphere excited by electric dipole source

We consider the emitter as an electric point dipole, and its dipole moment can be expressed as $\mathbf{p} = \hat{\theta}\, p\, \delta(r - r_s)\delta(\theta)\delta(\phi)$, where p is the magnitude of the dipole moment, and $r_s = a + d$ with the radius a of the silicon nanosphere (SiNS) locating at the origin of spherical coordinate (r,θ,ϕ) and the distance d between the dipole and the surface of the SiNS. The time-harmonics of the electromagnetic fields are assumed to be $e^{i\omega t}$. Consequently, the incident electric field of the electric dipole can be expressed in the spherical coordinate as[1]:

$$\mathbf{E}^i = \begin{bmatrix} E_r \\ E_\theta \\ E_\phi \end{bmatrix} = \begin{bmatrix} \frac{1}{i\omega\varepsilon}\frac{\partial^2}{\partial r^2}r + \frac{1}{i\omega\varepsilon}k^2 r & 0 \\ \frac{1}{i\omega\varepsilon}\frac{1}{r}\frac{\partial^2}{\partial r\partial\theta}r & \frac{1}{\sin\theta}\frac{\partial}{\partial\phi} \\ \frac{1}{i\omega\varepsilon}\frac{1}{r\sin\theta}\frac{\partial^2}{\partial r\partial\phi}r & -\frac{\partial}{\partial\theta} \end{bmatrix} \begin{bmatrix} \pi^e \\ \pi^m \end{bmatrix},$$

where ω is the angular frequency, k is the wavenumber, $\varepsilon = \varepsilon_0\varepsilon_r$ is the complex permittivity, π^e and π^m are the Debye potentials. Specifically, the Debye potentials can be written as:

$$\pi^e = p\frac{k}{i}\frac{\partial}{\partial\theta'}\frac{1}{r'}\frac{\partial}{\partial r'}r'\sum_{n=1}^{\infty}\frac{A_n(\theta,\phi,\theta',\phi')}{n(n+1)}j_n(kr_<)h_n^{(2)}(kr_>),$$

$$\pi^m = -i\omega\mu p\frac{k}{i}\frac{1}{\sin\theta'}\frac{\partial}{\partial\phi'}\sum_{n=1}^{\infty}\frac{A_n(\theta,\phi,\theta',\phi')}{n(n+1)}j_n(kr_<)h_n^{(2)}(kr_>),$$

where $\mu = \mu_0\mu_r$ is the complex permeability, (r',θ',ϕ') is the location coordinate of the dipole,

$A_n(\theta,\phi,\theta',\phi') = \frac{1}{4\pi}\sum_{m=-n}^{n}\frac{(2n+1)(n-|m|)!}{(n+|m|)!}e^{-im(\phi-\phi')}P_n^{|m|}(\cos\theta)P_n^{|m|}(\cos\theta')$ with the spherical Bessel function j_n and spherical Hankel function $h_n^{(2)}$, P_n^m is the associated Legend function, and $r_<\backslash r_>$ is the smaller\larger one of the position vectors of the source r_s and the observation point r, respectively. Particularly, for the dipole located at the point $(r_s,0,0)$, the Debye potentials can be written as:

$$\pi^e = -\frac{1}{4\pi}\frac{pk}{i}\frac{1}{r'}\frac{\partial}{\partial r'}\sum_{n=1}^{\infty}\frac{(2n+1)}{n(n+1)}r' j_n(kr_<)h_n^{(2)}(kr_>)P_n^1(\cos\theta)\cos\phi\,,$$

$$\pi^m = \frac{1}{4\pi}\omega\mu pk\sum_{n=1}^{\infty}\frac{(2n+1)}{n(n+1)}j_n(kr_<)h_n^{(2)}(kr_>)P_n^1(\cos\theta)\sin\phi\,.$$

Accordingly, the electric field inside the SiNS can be expressed as:

$$\mathbf{E}^c = \begin{bmatrix}E_r\\E_\theta\\E_\phi\end{bmatrix} = \frac{1}{4\pi}\begin{bmatrix}\frac{1}{i\omega\varepsilon_1}\frac{\partial^2}{\partial r^2}r+\frac{1}{i\omega\varepsilon_1}k_1^2 r & 0\\ \frac{1}{i\omega\varepsilon_1}\frac{1}{r}\frac{\partial^2}{\partial r\partial\theta}r & \frac{1}{\sin\theta}\frac{\partial}{\partial\phi}\\ \frac{1}{i\omega\varepsilon_1}\frac{1}{r\sin\theta}\frac{\partial^2}{\partial r\partial\phi}r & -\frac{\partial}{\partial\theta}\end{bmatrix}\begin{bmatrix}-\frac{pk_1}{i}\frac{1}{r_s}\sum_{n=1}^{\infty}\frac{(2n+1)}{n(n+1)}C_n^{(3)}j_n(k_1r)\left[r_s h_n^{(2)}(k_1r_s)\right]' P_n^1(\cos\theta)\cos\phi\\ \omega\mu_1 pk_1\sum_{n=1}^{\infty}\frac{(2n+1)}{n(n+1)}C_n^{(4)}j_n(k_1r)h_n^{(2)}(k_1r_s)P_n^1(\cos\theta)\sin\phi\end{bmatrix},$$

and the electric field scattered by the SiNS can be expressed as:

$$\mathbf{E}^s = \begin{bmatrix}E_r\\E_\theta\\E_\phi\end{bmatrix} = \frac{1}{4\pi}\begin{bmatrix}\frac{1}{i\omega\varepsilon_0}\frac{\partial^2}{\partial r^2}r+\frac{1}{i\omega\varepsilon_0}k_0^2 r & 0\\ \frac{1}{i\omega\varepsilon_0}\frac{1}{r}\frac{\partial^2}{\partial r\partial\theta}r & \frac{1}{\sin\theta}\frac{\partial}{\partial\phi}\\ \frac{1}{i\omega\varepsilon_0}\frac{1}{r\sin\theta}\frac{\partial^2}{\partial r\partial\phi}r & -\frac{\partial}{\partial\theta}\end{bmatrix}\begin{bmatrix}-\frac{pk_0}{i}\frac{1}{r_s}\sum_{n=1}^{\infty}\frac{(2n+1)}{n(n+1)}C_n^{(1)}\left[r_s h_n^{(2)}(k_0r_s)\right]' h_n^{(2)}(k_0r)P_n^1(\cos\theta)\cos\phi\\ \omega\mu pk_0\sum_{n=1}^{\infty}\frac{(2n+1)}{n(n+1)}C_n^{(2)}h_n^{(2)}(k_0r_s)h_n^{(2)}(k_0r)P_n^1(\cos\theta)\sin\phi\end{bmatrix}.$$

By examining the boundary conditions for the component of the electric fields, the four coefficients $C_n^{(i)}$, $(i=1,2,3,4)$ can be determined. We have found that the four coefficients are similar to the conventional Mie coefficients derived in the case of plane wave scattered by nanoparticles but with some modifications[2]. For example, the scattering coefficients can be expressed as:

$$a_n^{dip} = \frac{(k_1/k_0)\,\psi_n(k_1a)\,\psi_n'(k_0a)\,\eta_1\eta_2 - \psi_n(k_0a)\,\psi_n'(k_1a)\,\eta_3\eta_4}{(k_1/k_0)\,\psi_n(k_1a)\xi_n'(k_0a)\,\eta_1\eta_2 - \xi_n(k_0a)\psi_n'(k_1a)\,\eta_3\eta_4},$$

$$b_n^{dip} = \frac{\psi_n(k_1a)\,\psi_n'(k_0a)\,\eta_1\eta_2 - (k_1/k_0)\,\psi_n(k_0a)\,\psi_n'(k_1a)\,\eta_3\eta_4}{\psi_n(k_1a)\,\xi_n'(k_0a)\,\eta_1\eta_2 - (k_1/k_0)\,\xi_n(k_0a)\,\psi_n'(k_1a)\,\eta_3\eta_4},$$

where $\psi_n(\rho) = \rho\, j_n(\rho)$ and $\xi_n(\rho) = \rho\, h_n^{(1)}(\rho)$ are the Riccati-Bessel functions, and the introduced modifications induced by the dipole are $\eta_1 = \rho\, h_n^{(1)}(\rho)|_{\rho=k_1(a+d)}$, $\eta_2 = \left[\rho\, h_n^{(1)}(\rho)\right]'|_{\rho=k_0(a+d)}$, $\eta_3 = \rho\, h_n^{(1)}(\rho)|_{\rho=k_0(a+d)}$, $\eta_4 = \left[\rho\, h_n^{(1)}(\rho)\right]'|_{\rho=k_1(a+d)}$. For a fixed distance between the dipole and the SiNS, these modifications are constants. Therefore, the scattering efficiency is:

$$Q_{scat}^{dip} = \frac{2}{k_0^2 a^2}\sum_{n=1}^{\infty}(2n+1)\left(\left|a_n^{dip}\right|^2 + \left|b_n^{dip}\right|^2\right).$$

As can be seen in the equation above, the scattering efficiency of multipoles can be modified by the dipole compared to the case of plane wave scattering. These modified scattering efficiencies also has a distance-dependence introduced by the coefficients η_i $(i = 1,2,3,4)$ with the spherical Hankel function of dipole radiation. Therefore, the distance d between the dipole and the surface of the SiNS is also a critical parameter to minimize the contribution of electric dipole resonance, leading to pure magnetic dipole radiation. It should be noted that the constant coefficient differs from those in other works[3,4] is due to the fact that we have employed the modified Mie coefficients containing the coefficients η_i $(i = 1,2,3,4)$. When the dipole is far enough away from the SiNS, the coefficients η_i can be cancelled because the spherical Hankel function is asymptotically given by $h_n^{(1)}(kr) \sim \frac{(-i)^n e^{ikr}}{ikr}$, $kr \gg n^2$. Therefore, the scattering property of dipole radiation by the SiNS approaches the case of plane wave illumination.

5. The evolution of different emission multipoles with varying particle-emitter distances

To distance between the Si nanoparticle and a nearby ED emitter could affect the coupling strengths of the different particle multipoles and the emitter. To investigate this effect, we vary the particle-emitter distance (d), as illustrated in Fig. S4f, and inspect the evolutions of the different emission multipoles. Fig S4 show the multipole expansion of the total emission of an EDcSiNS with varying d. We see that the total emission is dominated by the MD and MQ modes, both of which exhibit weak dependence on d in the range of $1 - 10\ nm$. Particularly, the mode-purity factor of the MD resonance (δ_{md}) demonstrates low sensitivity to d, showing a $\delta_{md} > 0.99$ even at relatively large distance (Fig. S4f), say, $d = 10\ nm$.

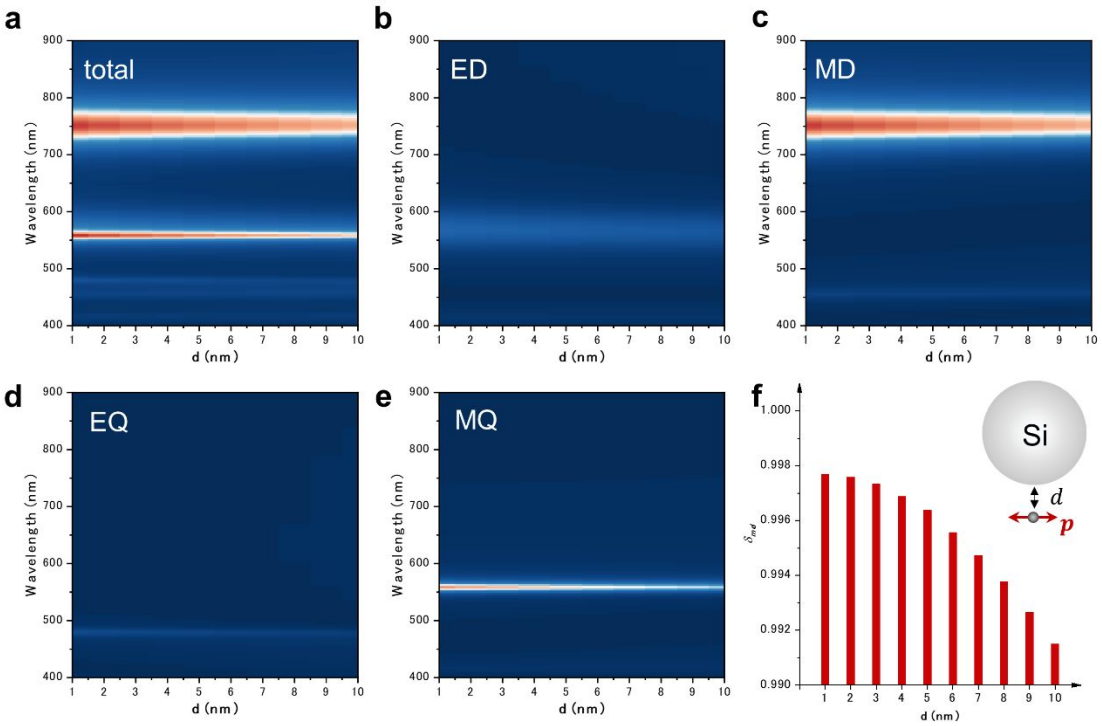

Figure S4. (a) The emission spectrum of an EDcSiNS with varying particle-emitter distance d. (b-e) The multipole expansion of the total emission shown in (a), mainly including the ED (b), MD (c), EQ (d) and MQ (e) components. (f) The evolution of the mode-purity-factor of the MD mode (δ_{md}) of an EDcSiNS with varying particle-emitter distance (d).

6. The modification of the dielectric substrate of the multipolar scattering and emission responses of a silicon nanoparticle

In experiment, silicon nanoparticles are usually placed on a dielectric substrate, which could modify the nanoparticle resonances. As shown in Fig. S5a, the silica substrate induces significant magnetoelectric coupling at the MD resonance wavelength[5], manifesting as a weak peak in the ED spectrum. However, this magnetoelectric coupling is marginal for the emission multipoles excited by a near-surface electric dipole (Fig. S5b), and the total emission character is not significantly modified by the dielectric substrate with respect to the EDcSiNS in air (Fig. 1d).

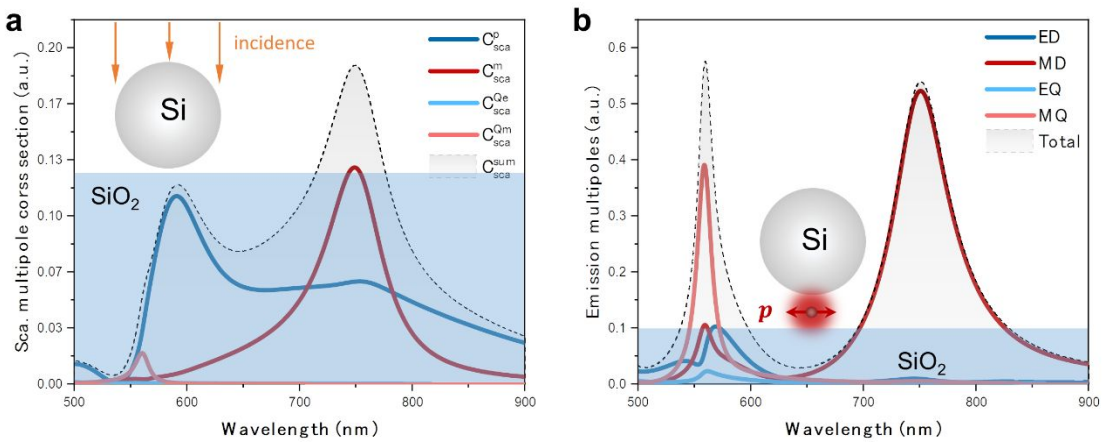

Figure S5. The scattering (a) and emission (b) multipoles of a silica-supported silicon nanoparticle (diameter 190 nm) illuminated by a plane wave and an electric dipole (transversely polarized) near the surface, respectively. The nanoparticle-substrate distance is 2 nm and the electric dipole source is located in the middle of the gap.

7. Experimental setup

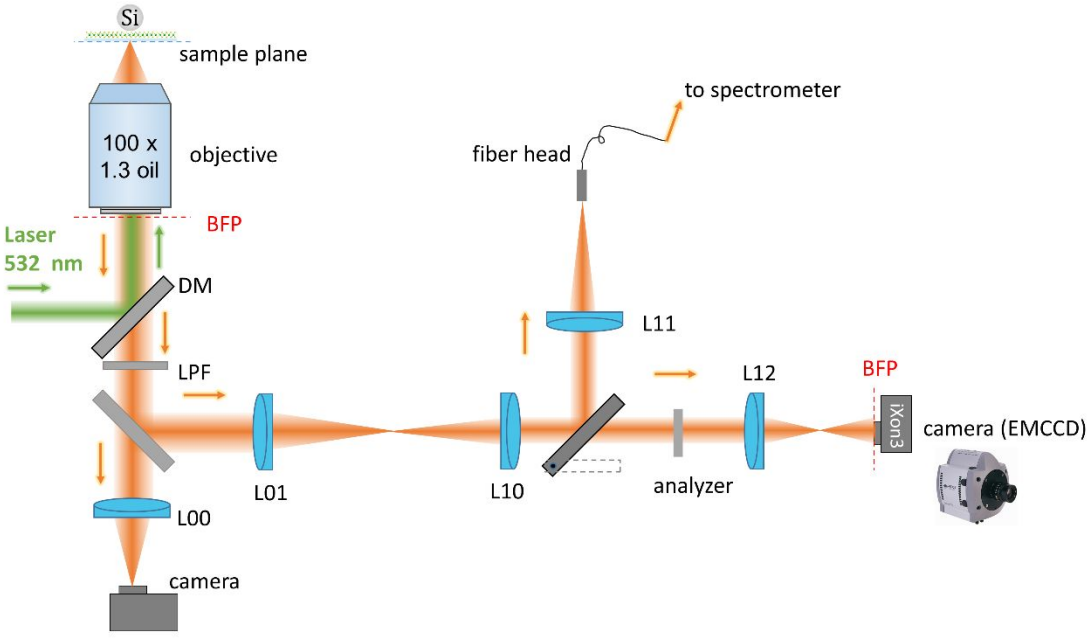

Figure S6. Experimental setup. BFP: back focal plane , DM: dichroic mirror, LPF: long-pass filter, L00-L12: lens and EMCCD: electron multiplying charge-coupled device (image sensor or camera). The multi-mode fiber is connected to a spectrometer and delivers the photoluminescence signal for spectral analysis.

Recording the back focal images of individual emitting nanostructures usually requires highly sensitive, low dark-current CCD cameras. Here we used an electron-multiplied CCD camera (iXon3)

from Andor, Inc. It features extremely low dark noises and high quantum efficiency at the detection wavelength range. Besides, we set longer exposure time (0.5s) for measuring the BFI images of etched EDcSiNS (Fig. 4d) with respect to their unetched counterparts (0.1s, Fig.4e), because the emission from etched sample contains only the WSe_2 emission coupled to the Si nanoparticles, much weaker than that of the etched one containing both coupled and uncoupled WSe_2 emission.

8. The emission of monolayered WSe2 off-resonantly coupled to a silicon nanoparticle

When the structural MD resonance of a hybrid SiNS-WSe_2 structure doesn't match the exciton wavelength of the WSe_2, the emission character of the WSe_2 will be modified and tuned to the same wavelength of the MD resonance, as shown in Fig S7a, b. Besides, the emission patterns of such off-resonantly coupling structures exhibit clear MD characters as for their resonantly coupled counterparts (Fig. S7c, d), i.e., the two-lobes-shaped emission profiles orienting along the transmission axis of the analyzer (T_x). These observations agree well with the simulation results shown in Fig.S8, in which the electric dipole emission at wavelength far from the MD resonance peak of the Si nanoparticle (see the insets in Fig. S8 showing the case for 650 and 850 nm) still preserves dominant MD characters in their radiation profiles.

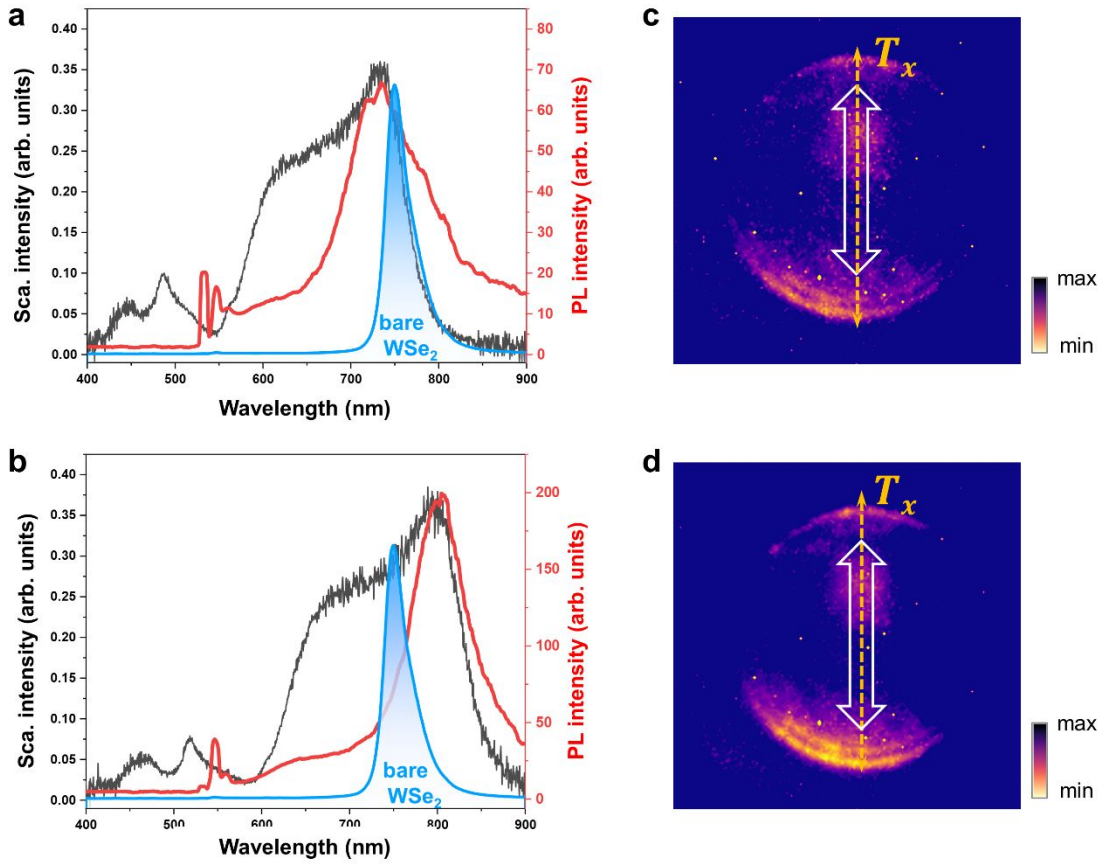

Figure S7. The emission characters of the WSe_2 monolayer off-resonantly coupled to a Si

nanoparticle. (a, b) The emission spectra (red) of two hybrid SiNS-WSe_2 structures which show MD resonances significantly deviate from the excitonic wavelength of monolayered WSe_2.The scattering spectra (black) of the hybrid structures, as well as the emission spectra of bare WSe_2 monolayers (shadowed blue) are also shown for reference. (c, d) The corresponding emission patterns of the structures in (a, b).

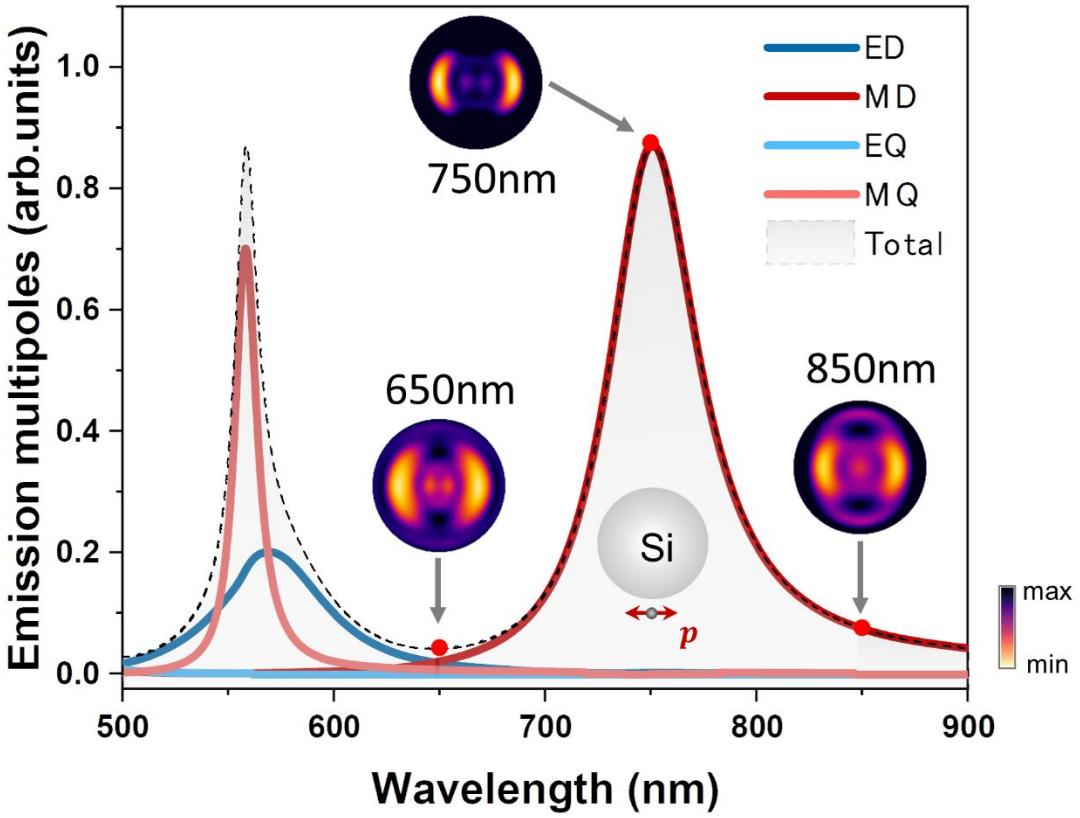

Figure S8. Multipole expansion of the emission of an EDcSiNS and simulated emission patterns at different wavelengths. The particle diameter is 190 nm, and the emitter-surface distance is 1 nm.

REFERENCES

(1) Okhmatovski, V. I.; Cangellaris, A. C. Efficient Calculation of the Electromagnetic Dyadic Green~s Function in Spherical Layered Media. *IEEE Trans Antennas Propag* **2003**, *51* (12), 3209–3220. https://doi.org/10.1109/TAP.2003.820952.

(2) Bohren, C. F. *Absorption and Scattering of Light by Small Particles*; 1983. https://doi.org/10.1088/0031-9112/35/3/025.

(3) Yao, K.; Zheng, Y. Directional Light Emission by Electric and Magnetic Dipoles near

a Nanosphere: An Analytical Approach Based on the Generalized Mie Theory. *Opt Lett* **2021**, *46* (2). https://doi.org/10.1364/ol.411352.

(4) Schmidt, M. K.; Esteban, R.; Sáenz, J. J.; Suárez-Lacalle, I.; Mackowski, S.; Aizpurua, J. Dielectric Antennas - a Suitable Platform for Controlling Magnetic Dipolar Emission. *Opt Express* **2012**, *20* (13). https://doi.org/10.1364/oe.20.013636.

(5) E. Miroshnichenko, A.; B. Evlyukhin, A.; S. Kivshar, Y.; N. Chichkov, B. Substrate-Induced Resonant Magnetoelectric Effects for Dielectric Nanoparticles. *ACS Photonics* **2015**, *2* (10), 1423–1428. https://doi.org/10.1021/acsphotonics.5b00117.